Mixed Pluronics/phosphatidylcholine self-assemblies for curcumin drug for antimicrobial evaluations

4.1: Introduction

Natural plant products have been used in a wide range of complementary and alternative medicine (CMA) therapies and diagnostic studies. Natural products have the advantage of being effective and benign, and they can be administered at therapeutic dosages much lower than their toxic levels[1]. The solid gold of India Turmeric is a natural flowering plant belonging to the perennial herb family, Curcuma longa. CUR, a polyphenol taken from the herb Curcuma longa's rhizome, exhibits a variety of biological and pharmacological activities[2,3]. CUR is a diarylheptanoid comprised of two aromatic rings joined by a seven-carbon chain. It contains two ortho-methoxy phenol groups, two enone groups, and a keto-enol moiety, among other functionally active groups. It's a lipophilic polyphenol that can be dissolved in organic solvents and also in alkali or extremely acidic mediums. The keto-form is the dominant form at neutral and acidic pH levels, as well as in cells. The enol form, on the other hand, dominates at alkali pH, where CUR releases electrons in a mechanism that shows its antioxidant scavenging properties. CUR's structure is stabilized through resonance-guided H-bonding in the enol form [4]. On the Asian continent and specifically India, CUR has been used for a period of years to cure several disorders due to its antioxidant, anti-inflammatory, antiseptic, antimicrobial, anticoagulant, wound healing, and anticarcinogenic properties[5,6]. Research on animal and human models presented the safety of CUR even at a large dosage (8 g/day) [7]. However, its therapeutic uses are limited owing to its poor water solubility, instability against light and lipophilic properties, all of which result in pharmacokinetic problems such as low absorption, below par bioavailability, extensive metabolism, and rapid elimination [7,8]. Enhancing CUR solubility and stability is still an important and basic requirement for highly desired oral bioavailability.

Many drug carriers have been studied in order to improve CUR drug absorption and efficacy, and nanovehicles hold great promise [9]. Encapsulating hydrophobic drugs into polymeric micelles as nanovehicles is an effective approach for the improvement of drug solubility and better bioavailability[10,11]. As a nanovehicle, polymeric micelles based on amphiphilic triblock copolymeric surfactant PEO-PPO-PEO, commercially available as Pluronic, show potential as candidates for improved bioavailability of water-insoluble drugs[12,13]. Many Pluronics are FDA approved pharmaceutical excipients[14]. Pluronic

micelles have a core-corona structure that provides significant benefits, such as drug targeting, ease of production, and long circulation. However, the poor stability of such Pluronic micelles in the cardiovascular system or GI fluids, as well as the eventual drug precipitation, prohibits their application in the delivery of drugs. Therefore, the mixed Pluronic micelles have been significantly studied for the enhanced oral bioavailability of lipophilic drugs. Pluronic mixed micelles made of thermally stable hydrophobic Pluronic and kinetically stable hydrophilic Pluronic performed exceptionally well in drug solubilization and stability, paving the way for much more effective pharmaceutical applications[15-22]. Pluronic mixed micelles increase the volume of the PPO core of respective micelle by combining extra materials with hydrophobicity, furnishing a larger solubilization site for water-insoluble drugs. It also retains all the benefits of single Pluronic micelles while enhancing the solubilization capacity for hydrophobic drugs.

Pluronics have been extensively functionalized to produce drug delivery nanovehicles that have active targeting, stimuli responsiveness, and high drug loading capacity. To develop a more potent Pluronic mixed nanomicellar system for drug delivery, many biocompatible compounds are combined. The combination of highly biocompatible compounds like PC with Pluronic mixed nanomicelles plays a significant role in nanoparticle drug delivery. These Pluronics/PC mixed micellar systems offer various advantages for improving therapeutic efficacy in addition to drug solubilization[23-25]. PC, a naturally occurring phospholipid, is a nontoxic and biocompatible material that has been used by food and pharmaceutical companies[26]. The compatibility of the PC with human membranes and skin is the first and most important advantage of a PC-based vesicular system. Hence, PC based formulations improve the therapeutic efficacy of lipophilic drugs[27].

In this context, the current study was aimed to develop and characterize the Pluronic/PC mixed nanomicellar formulations for improved insolubility and bioavailability of the CUR drug. We investigated the oral bioavailability of CUR using Pluronic/PC mixed nanomicellar formulations composed of the highly hydrophobic Pluronic P123, the hydrophilic Pluronic F68, and PC coded as PFPC. The RSM was used to optimize PFPC mixed nanomicellar formulation. The RSM, in combination with D-optimal design, is a systematic way of designing, optimizing, and delivering any active pharmaceutical substance or process[28]. The D-optimal design is a fast method for finding the impact of independent

variables on each dependent variable. The optimal formulation has been determined using ANOVA regression analysis. The particle size, zeta potential, PDI, morphology, and solubility of the optimized CUR-incorporated P123/F68/PC mixed micellar formulation (coded as CUR-PFPC) were examined using UV-Vis, DLS, and TEM measurements. The biocompatibility and stability of the mixed nanomicellar formulation were examined through FTIR, XRD, and DSC analysis. Also, the CUR drug release and antioxidant behaviour of CUR and CUR-PFPC nanoformulations were evaluated *in vitro*. Furthermore, the antibacterial and antifungal assays of CUR and CUR-PFPC nanoformulations were investigated opposed to Gram-positive bacteria, Gram-negative bacteria, and fungi. Thus, our findings present a concise approach for the Pluronic/PC mixed naomicellar formulations as the nanovehicles that could enhance the solubility, oxygen resistance, and antimicrobial effects of CUR.

4.2: Experimental Section

4.2.1: Optimization and fabrication of PFPC and CUR-PFPC mixed polymeric micellar formulations

4.2.1.1 Statistical optimization through D-optimal design

The current research used the D-optimal design to optimize the PFPC, and CUR-PFPC mixed nanomicellar formulation methods. Facilitated by mathematical software, RSM is an illustrious tool for optimization in pharma to help extract valuable information from a few well-designed experiments. CUR-PFPC mixed micellar formulations were prepared as per the 3-factor D-optimal design using Design-Expert software to evaluate the influence of variables on the micellar characteristics[29]. Using D-optimal design, the contributions of the influential variables, comprising the concentration of P123(A), F68(B), PC(C), and the amount of CUR (D), were estimated based on the solubility, %DL, and %EE. The independent variables and their levels examined dependent variables, and their code classes of −1 and +1 are tabulated in Table 4.1. The composition of the 25 runs of the D-optimal design is listed in Table 4.2. The 3D surfaces and contour graphs investigated the effects of different variables on responses. The ANOVA analysis determined P-values, F-values, and model F-values for each factor and observed the P-values of <0.05.

Table 4.1. The labels and limits of independent and dependent variables applied in the experimental design

Label	Independent variables	Unit	Lower limit (coded as -1)	Upper limit (coded as +1)
A	Concentration of P123	%w/v	0	5
B	Concentration of F68	%w/v	0	5
C	Concentration of PC	%w/v	0	1
D	Amount of drug	mg	2	20
Dependent variables				
Y1: Solubility (mg/mL)			Maximize	
Y2: %DL			Maximize	
Y3: %EE			Maximize	

Table 4.2. Experimental runs and results based on D-optimal design.

Run	Independent variables				Dependent variables (Responses)		
	A	B	C	D	Y1	Y2	Y3
1	4.61	0.00	0.79	18.3	0.0459	4.8377	6.2636
2	0.00	2.56	1.00	2.00	0.0085	3.8219	10.625
3	3.28	5.00	0.10	2.28	0.0450	10.553	49.342
4	0.00	2.48	0.48	10.8	0.0021	0.3799	0.4834
5	5.00	5.00	0.10	20.0	0.0537	4.4601	6.7125
6	2.52	2.34	0.56	20.0	0.0220	2.1636	2.7500
7	0.00	0.00	1.00	20.0	0.0119	1.4166	1.4875
8	0.00	0.00	0.36	2.00	0.0041	4.3432	5.1250
9	5.00	2.40	0.55	11.0	0.0534	7.0152	12.048
10	5.00	0.00	1.00	2.00	0.0519	16.218	64.875
11	2.12	0.16	0.78	9.63	0.0257	5.0634	6.6718
12	5.00	5.00	1.00	2.00	0.0735	14.134	91.875
13	0.00	5.00	1.00	20.0	0.0056	0.5384	0.7040
14	0.00	2.21	0.10	20.0	0.0057	0.6387	0.7125
15	5.00	3.15	1.00	20.0	0.0454	3.8936	5.6850
16	2.11	5.00	0.55	20.0	0.0231	2.0878	2.8875
17	5.00	2.21	0.10	9.83	0.0388	5.6924	9.8677
18	0.00	5.00	0.10	2.00	0.0011	0.3873	1.3750
19	0.00	5.00	1.00	20.0	0.0026	0.2500	0.3250
20	2.21	0.00	0.10	9.95	0.0217	4.4240	5.4523
21	0.00	0.00	0.36	2.00	0.0041	4.3432	5.1250
22	5.00	5.00	0.10	20.0	0.0486	4.0365	6.0750
23	0.00	2.56	1.00	2.00	0.0024	1.0791	3.1000
24	5.00	0.00	0.10	20.0	0.0365	3.6354	4.5625
25	5.00	5.00	1.00	2.00	0.0733	14.096	91.625

4.2.1.2 Fabrication of PFPC and CUR-PFPC mixed polymeric nanomicellar formulations

PFPC nanomicelles formulations were fabricated by the fine-film hydration method at different concentrations according to the experimental design. First, solubilize the P123, F68, and PC in chloroform to get uniform stock solutions. Then, the necessary volume of the stock solution of P123, F68, and PC was transferred in a RBF with appropriate dilution. After that, the solvent was slowly removed at 60°C under reduced pressure in a rotary evaporator (R-100-labindia, India) to obtain a thin, dry film. Then, the flask was kept overnight in a vaccum at RT to dry the residual solvent from the film. Then, the fine film was hydrated with the necessary amount of distilled water, sonicated for 10 min, and filtered through nylon membrane to obtain a PFPC mixed micellar dispersion. Finally, the micelles formulation was solidified by freeze-drying. The same procedure was followed for the preparation of the

CUR-PFPC nanomicelles formulations by taking the drug as per the experimental design along with the Pluronics and PC.

4.2.1.3 Formulation optimization

The optimized CUR-PFPC mixed nanomicellar formulation was evaluated using the Design Expert® software. The optimized CUR-PFPC nanoformulation finally came out was then prepared and investigated to confirm the authenticity of the calculated optimal formulation factors and estimated responses produced by the program.

4.2.2 Characterization methods

Mixed micellar size, zeta potential, and morphological investigations of PFPC and CUR-PFPC were characterized using DLS and TEM. CUR compatibility and stability in mixed micellar formulation investigated using FTIR, XRD, DSC and UV-Vis spectroscopy techniques. The detailed procedure of the all-mentioned techniques is shown in Chapter 2.

4.2.3 *In-vitro* biological investigations

4.2.3.1 In-vitro % drug release

The release of CUR from CUR-PFPC mixed nanomicellar formulation was investigated using the dialysis method in phosphate buffer solution (PBS, pH 7.4)[30]. The dialysis membrane was activated and dipped in the release medium overnight before the *in-vitro* dissolution study. The CUR-PFPC mixed micellar formulation was filled into the end sealed dialysis membrane tube. The membrane was sink in 100 mL of fresh PBS in a 250 mL glass container and maintained at a constant temperature of 30±0.2°C. The sample solution (4 mL) was taken from the release medium at a pre-decided time and replaced with the same volume of freshly prepared PBS to maintain the sink condition. The sample solutions were diluted, and the released CUR amount was found by analyzing the absorbance at a λmax of 425 nm using a UV-Vis spectrophotometer. The cumulative % release of CUR in the medium was calculated with the help of a calibration curve. The drug release profile of CUR was plotted as the cumulative amount of CUR released against time. The experiment was performed in the dark and in triplicate to get the mean value. CUR drug release study was also conducted in the same manner to evaluate nanoformulation performance better.

4.2.3.2 In-vitro Antioxidant Assay

The oxygen resistance (%) of the optimized CUR-PFPC mixed nanomicellar formulation with different concentrations (1.0, 5.0, 10.0, 15.0, 20.0, and 25.0 µg/mL) was assessed by investigating their ability to DPPH radical scavenging. The sample solutions were properly mixed and left for 1½ hrs in a dark place at RT for incubation. DPPH accepts electrons, and the sample color changed from deep violet to light yellow, indicating the formation of DPPH-H (non-radical) in the medium and measured by a UV-Vis spectrophotometer (λmax of 517 nm). The DPPH scavenging potential of the examined samples was determined by comparison of the sample color with that of the control[31]. The experiments were done thrice to get the mean value. The inhibition percentage was calculated using the equation (3):

$$\% \text{ Oxygen resistance} = (A0-A1)/A0\times 100\ldots\ldots (1)$$

Where A0 = Control and A1 = Sample present

The result was evaluated in IC_{50} values, the amount of oxygen resistance necessary to decrease 50% of the DPPH initial concentration.

4.2.3.3 In-vitro antimicrobial activity

In vitro antimicrobial (antibacterial/antifungal) activity was carried- out using the agar well diffusion technique[32]. The pure CUR, PFPC and optimized CUR-PFPC nanomicellar formulation were poured (100µL) into wells (7mm) of sterile nutrient agar plates then inoculated with Gram-positive Staphylococcus aureus (S. aureus) and Bacillus subtilis (B. subtilis), and Gram-negative Escherichia coli (E. coli) and Pseudomonas aeruginosa (P. aeruginosa) bacteria. In another antifungal study, Penicillium, Aspergillus niger (A. niger), and Saccharomyces cerevisiae (S. cerevisiae) were selected. Both bacteria and fungi were grown in sterile nutritive agar and potato dextrose agar media. The culture media was sterilized in an autoclave at 15 lb per inch pressure at the 121°C temperature for 15 min. After that, they cooled down to 40°C, and the agar solutions (~20 mL) were spilled into sterile Petri dishes and solidified. Next, the strains were swabbed on the agar using sterile cotton. The sample discs utilized in this process had a 7 mm diameter (~30 µg sample). After that, the test solution of 50µl each was poured into each well of the Petri-dishes. After conceding the diffusion of optimized CUR, PFPC and CUR-PFPC mixed nanomicellar formulation for 2 hrs for analysis, and the reacted agar plates were incubated at

37°±0.5°C for 24 h for antibacterial and 5 days at 25°±2°C for antifungal activity. The antibacterial and antifungal activities were evaluated by measuring the diameter (mm) of the inhibition zone around each well and sample disc using a Vernier caliper. The entire process, only the incubation part, was done in a laminar flow unit[33,34]. Each experiment was performed thrice to get the mean value.

4.2.3.4: Statistical analysis

Data were presented as mean value ± standard deviation (SD). The experiments were performed in triplicate to get a mean value ± SD. SPSS 22.0 software was used to compare data. $p \leq 0.05$ or less was considered as a statistically significant.

4.3: Results and discussion

Assembling drug-loaded mixed Pluronic/PC micelles is a complex procedure and usually requires various materials and methods of preparation. Moreover, its commercialization is challenging due to a lack of scale-up data and regulatory issues. Apart from these development issues, inadequate guidelines on shelf-life, bioavailability, and impurities are barriers to commercialization and need formulation novelty. The QbD is the latest trend to develop and optimize various significant pharmaceutical processes. According to QbD, quality should build into products rather than only be assessed after manufacturing[35]. Applying QbD principles in drug-loaded Pluronic/PC mixed micelles is expected to help overcome existing issues with Pluronic/PC mixed micellar formulations, start providing wider regulatory acceptance, and accelerate clinical application.

4.3.1 Statistical analysis of the D-optimal design

Table 4.3: The ANOVA regression analysis of variance results of the fitted model for all the responses

Response	**Y1**: Solubility (mg/mL)	**Y2**: %DL	**Y3**: % EE
Model	2FI	Quadratic	Quadratic
R^2	0.9823	0.9809	0.9836
Adjusted R^2	0.9696	0.9541	0.9605
Predicted R^2	0.9403	0.8214	0.7955
Adequate Precision	26.129	22.278	24.313
Significant terms (p-value)	A(<0.0001), B(0.0014), C(0.0172), D (0.0074), AB (0.0005), AD(0.0069)	A(<0.0001), D(<0.0001), AD (<0.0001) D^2(0.0212)	A(<0.0001), B(<0.0001), C(0.0056), D (0.0149), AB (0.0343), AD(<0.0001), BD (0.0265) CD(0.0295), B^2(0.0381), D^2(0.0133)

RSM is a set of mathematical and statistical tools for modeling and properly analyzing difficulties in which a set of variables impacts the desired response to optimize the outcomes. A D-optimal design was used to optimize the CUR-PFPC mixed nanomicellar formulation in the present work. The three significant variables, solubility, %DL, and %EE, were selected to find the optimum CUR-PFPC mixed nanomicellar formulation using 25

experimental recipes. The ANOVA analysis confirms the adequacy of the model. The best fit for each response, Y1 (solubility), Y2 (%DL), and Y3 (%EE), was checked for normality and outliers. The various effects of model terms associated with the responses of regression variances are presented in Table 4.2. The F-ratio was used to compare the actual variation and the expected change regarding variable averages. The P-value < 0.05 indicates that the model was significant (Table 4.2). The value and sign of the quantitative effect show the magnitude and direction of the term's influence on the response. The positive (+) value in the equation shows that a variable has a positive impact on the response, while a negative (-) value demonstrates an antagonistic effect (inverse relationship) between the variable and the response[28, 36].

4.3.1.1 Solubility model analysis

The solubility (Y1) of CUR in CUR-PFPC mixed nanomicellar formulations was found to be 0.0011 to 0.0735 mg/mL (Table 4.2). The P-value of <0.0001 of the response Y1 suggested that such a model was significant. On the other hand, the F-value(lack of fit) of 2.53 indicates the lack-of-fit is non-significant, and such a higher value came due to noise. Generally, a non-significant lack-of-fit is better for the formulation. The 2FI equation that correlates the independent variables and the solubility is shown in equation (1).

$$\text{Solubility} = 0.0339 + 0.0194 * \text{A} + 0.0032 * \text{B} + 0.0030 * \text{C} - 0.0034 * \text{D} + 0.0035 * \text{A} * \text{B} + 0.0009 * \text{A} * \text{C} - 0.0029 * \text{A} * \text{D} - 0.0005 * \text{B} * \text{C} - 0.0017 * \text{B} * \text{D} - 0.0009 * \text{C} * \text{D} \quad \ldots\ldots(2)$$

Figure 4.1 displays the response surfaces from the interaction between the concentration of P123 (A), F68 (B), PC (C), and the amount solubilized of CUR drug (D), when solubility is counted. The contour plot shape indicated a significant interaction between all the independent variables. The positive sign of the A, B, and C coefficients showed a positive effect on the CUR solubility. The CUR solubility increased with the concentration of P123, F68, and PC as it created the large hydrophobic core of the mixed micelles. As proved by the negative coefficient of D in the experiment, the solubility of CUR significantly decreased with increasing levels of CUR.

4.3.1.2 %DL model analysis

The %DL (Y2) of the CUR-PFPC mixed nanomicellar formulation ~~at~~ was found to be 0.250 to 16.22% (Table 4.2). The F-value of 36.75 indicated that the %DL model was significant. With the Prob > F value less than 0.0500 (P = 0.0001), the model was significant. The F-value(lack of fit) of 1.36 suggested that the lack of fit was not significant and better for the system. The Pred R^2 of 0.8215 is quite a good accordance with the Adj R^2 of 0.9542. The highest %DL obtained at the optimized point was observed from the 3D response plots displayed in Figure 4.2. The final equation (3) for %DL is as follows:

$$\%\,\mathrm{DL} = 4.298 + 2.8230 * \mathrm{A} - 0.2232 * \mathrm{B} + 0.3172 * \mathrm{C} - 3.4030 * \mathrm{D} + 0.2579 * \mathrm{A} * \mathrm{B} + 0.1376 * \mathrm{A} * \mathrm{C} - 1.7250 * \mathrm{A} * \mathrm{D} - 0.1588 * \mathrm{B} * \mathrm{C} + 0.3622 * \mathrm{B} * \mathrm{D} - 0.2018 * \mathrm{C} * \mathrm{D} - 0.3209 * \mathrm{A}^2 + 0.4871 * \mathrm{B}^2 - 0.2177 * \mathrm{C}^2 + 1.9120 * \mathrm{D}^2 \ldots\ldots (3)$$

The (+) positive signs of A and C indicated that %DL significantly increased with an increase in the concentration of P123 (A) and PC (C) because of the highly hydrophobic nature of P123 and the support of PC, the volume of the hydrophobic core of the mixed micelles was increased, which ultimately favours the CUR drug loading. So, the negative coefficient of B and D indicated that %DL significantly decreased with increasing the concentration of F68 (B) and amount of CUR (D), respectively. Such antagonistic behavior correlated with the hydrophilic nature of the F68 polymers.

4.3.1.3 %EE model analysis

The other response, the incorporation efficiency of the formulation, was obtained in the range of 0.3250–91.4 %. The F-value of 41.49 involves that the model was significant. Values of Prob> F <0.0500 suggested that the model was significantly effective. The F-value(lack of fit) of 1.96 was non-significant and found good. To illustrate the effect of each independent variable on %EE, 3D response plots were drawn and are shown in Figure 4.3. The final polynomial equation in terms of coded factors that relate the independent variables and the drug incorporation efficiency obtained through software for % EE is as follows:

$$\%EE = 9.3890 + 11.770 * A + 5.9350 * B + 4.8600 * C - 19.420 * D + 2.5500 * A * B + 2.371 * A * C - 11.040 * A * D + 1.848 * B * C - 3.317 * B * D - 4.375 * C * D - 0.7650 * A^2 + 4.456 * B^2 - 1.378 * C^2 + 12.00 * D^2 \quad \ldots\ldots(4)$$

The positive sign against A, B, and C coefficient indicated that drug incorporation efficiency significantly increased with increasing concentration of P123, F68, and PC. The negative coefficient of D indicates that as drug levels increased, % EE decreased significantly. To illustrate the effect of each independent variable on dependent variable, 3D response plots were drawn which were indicated a significant interaction between all the independent variables and dependent variable. The signal-to-noise ratio was examined with adequate precision, and a value > 4 was desirable. In the cases of solubility, %DL, and %EE, the ratio values were 26.150, 22.330, and 23.962, respectively assures the ability of the model to navigate the design.

The prediction of statistical models has been validated through the experimental analysis. The predicted and experimental data of optimized formulation is listed in Table 4.**4**. With these optimization investigations, the mixed micellar formulations were prepared and analyzed for their practical outcomes for the better bioavailability of the CUR drug.

The prediction of statistical models has been validated through the experimental analysis. The predicted and experimental data of optimized formulation is listed in Table 4.4. With these optimization investigations, the mixed micellar formulations were prepared and analyzed for their practical outcomes for the better bioavailability of the CUR drug.

Table 4.4. The observed and the predicted values of the optimum CUR-PFPC mixed micellar formulation based on D-optimal design.

Dependent Variable	Predicted	Observed	Bias
Solubility (mg/mL)	0.0792	0.0713	-0.0079
% DL	12.4280	12.7820	-0.3540
% EE	90.1683	91.1713	-1.0030

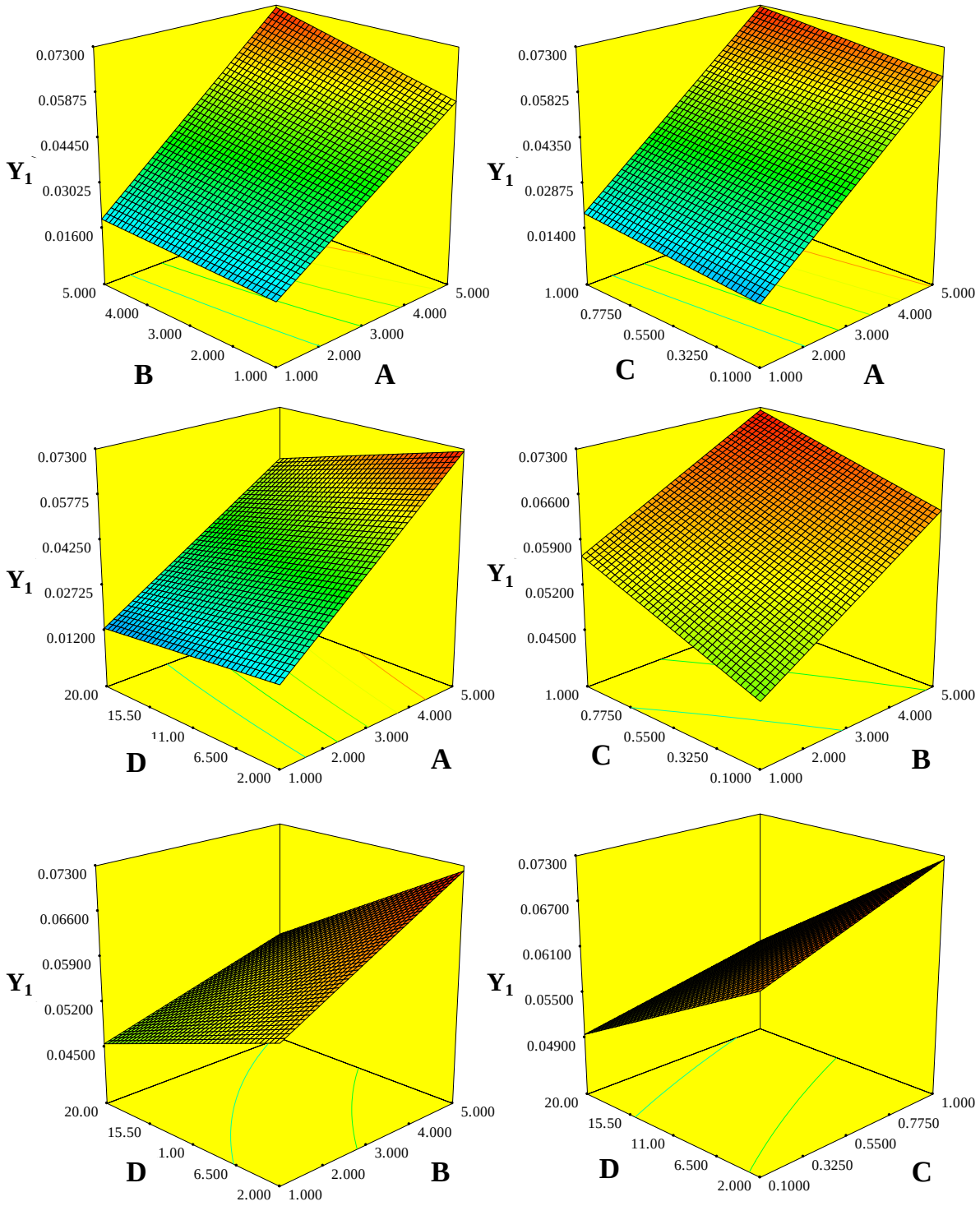

Figure 4.1: The 3D response surface plots for the effect of the respective independent variable on solubility

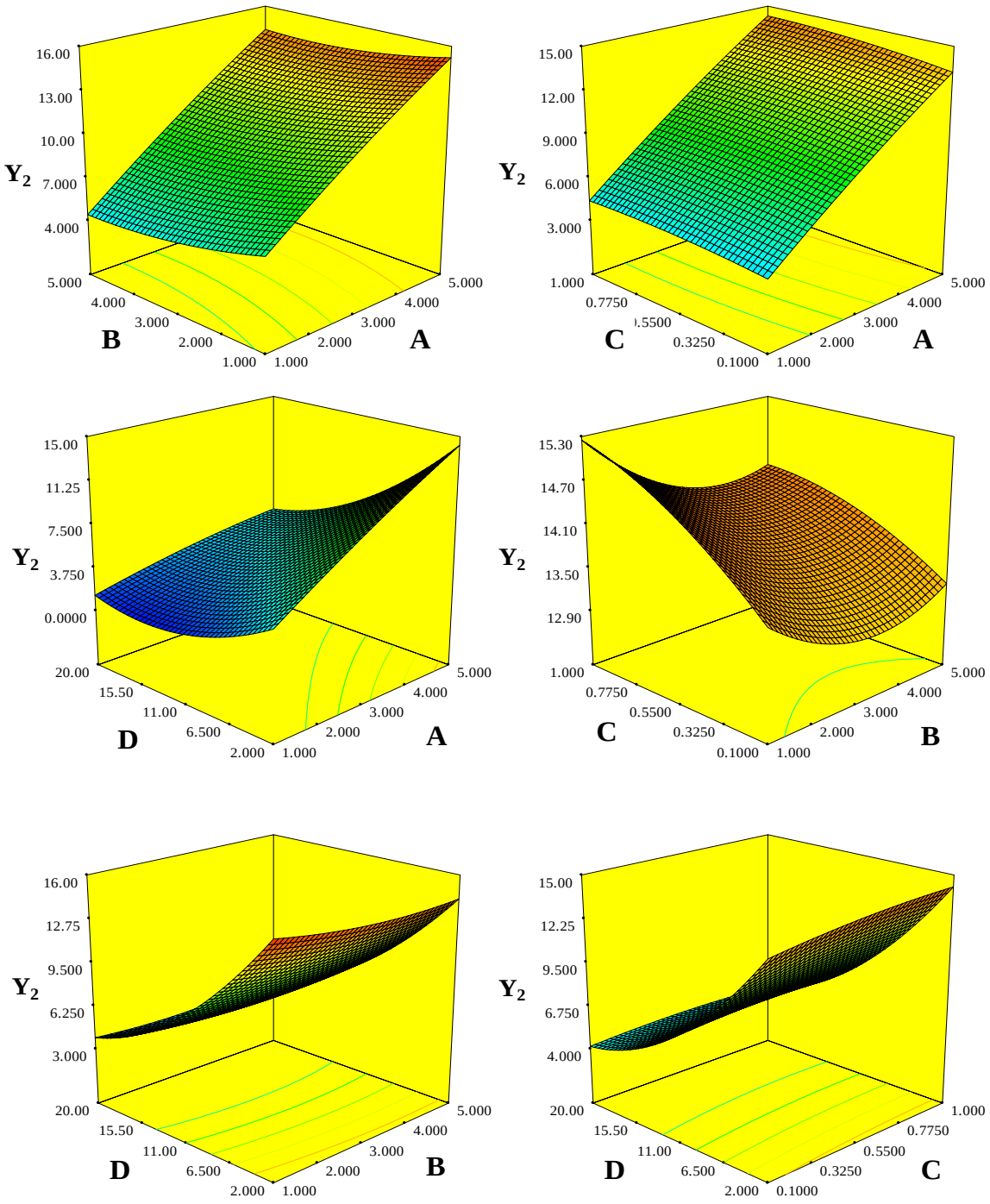

Figure 4.2: The 3D response surface plots for the effect of the respective independent variable on %DL

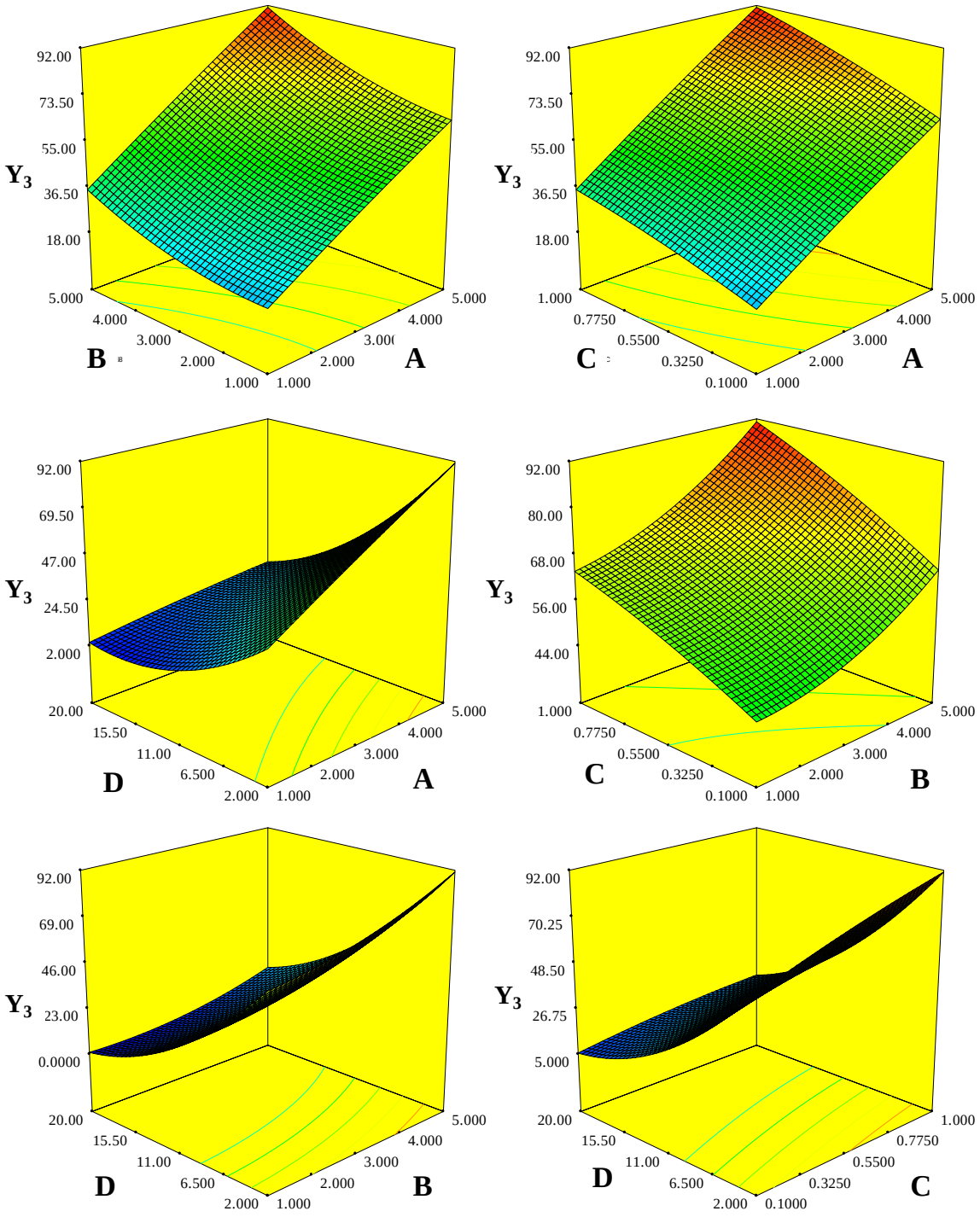

Figure 4.3: The 3D response surface plots for the effect of the respective independent variable on %EE

4.3.2: Characterization of PFPC and CUR-PFPC mixed nanomicellar formulations

4.3.2.1: Mixed micellar size, zeta potential, and morphological investigations

The DLS technique was employed to obtain the particle size of the optimized PFPC and CUR-PFPC mixed nanomicellar formulations in terms of apparent micellar hydrodynamic diameter (Dh) and PDI. The Dh of PFPC and CUR-PFPC mixed nanomicellar formulations were 59.79 nm and 67.43 nm, respectively (Figure 3(a)). Zhao et al.[20] reported the Dh of the mixed P123/F68 micellar system was 23.4 nm. Due to the inclusion of PC in the PFPC mixed micellar system, they significantly increased their Dh (here 59.79 nm) in comparison to the mixed P123/F68 micellar system. The Pluronic PPO chains and PC alkyl chains are assembled into a core of mixed micelles. Surrounding the hydrophobic core is a shell comprised of PC polar head groups and PEO of Pluronics.

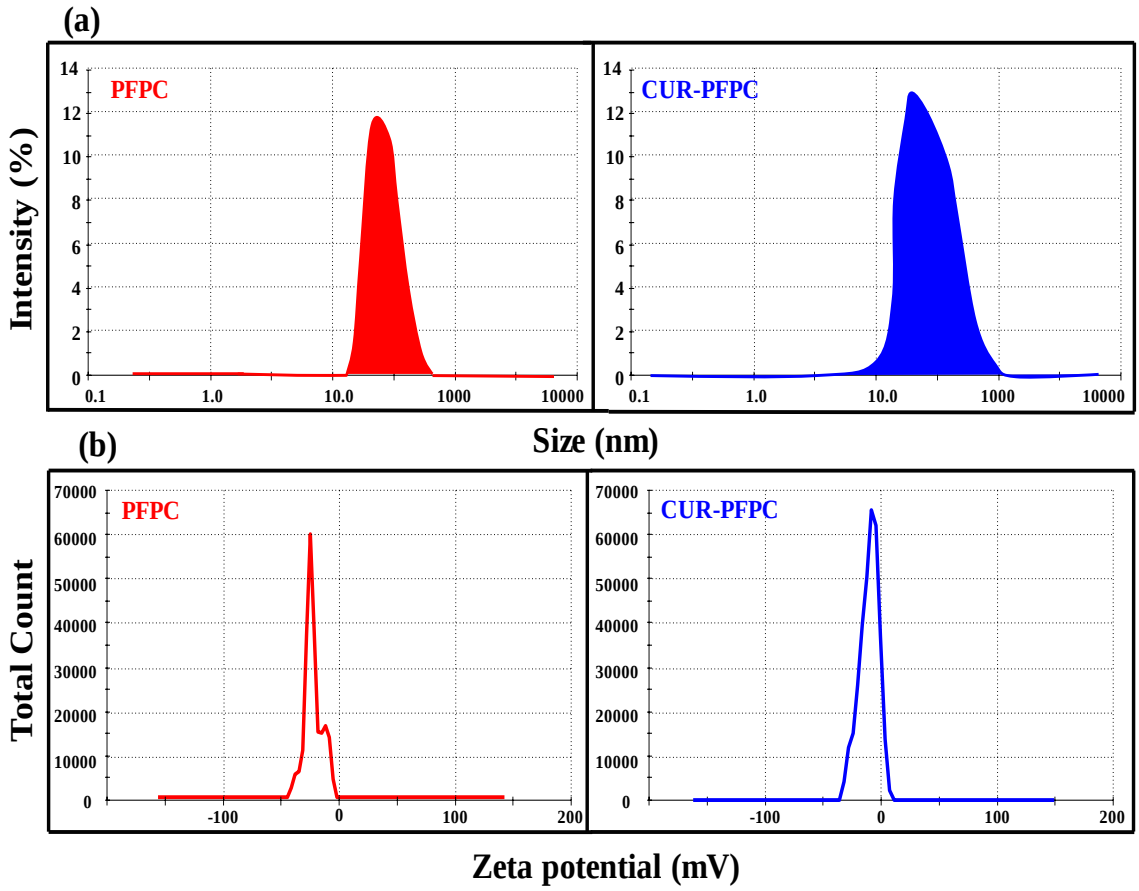

Figure 4.4: (a) Micellar size distribution, and **(b)** Zeta potential plots of optimized PFPC and CUR-PFPC formulations at 30°±0.5° C. Data are demonstrated as mean ± S.D (n=3).

The higher Dh of the CUR-PFPC nanomicellar formulation ($P < 0.05$) was accredited to the presence of the CUR in the lipophilic core of the mixed micelles. The PDI values of the PFPC and CUR-PFPC nanomicellar formulations were 0.469 and 0.528, respectively. The examined micellar formulations displayed a PDI <0.6, thereby indicating a low polydisperse populace of particles[37]. The PDI increases when micelles manifest substantial thickening or a hydrophobic additive is solubilized and fabricates mixed micelles. Hence, the PDI of CUR-PFPC increased with incorporating the CUR into the mixed micellar core of PFPC.

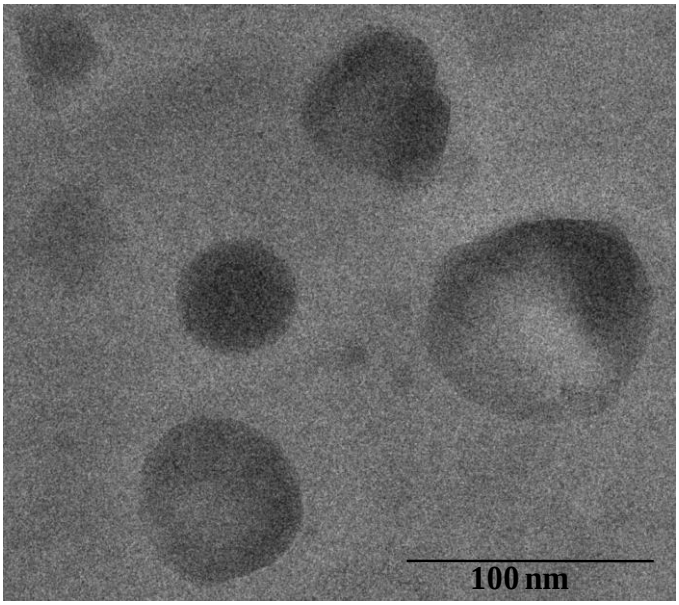

Figure 4.5: TEM micrograph of optimized CUR- PFPC formulation

The zeta potential of the particles dramatically influences the stability of a mixed micellar formulation. The low zeta potential value creates enough steric barriers or electric repulsion to prevent micellar aggregation[19]. The potential zeta values of the PFPC and CUR-PFPC mixed nanomicellar formulations were 16.2 mV and -15.1 mV, respectively (Figure 4.4(b)). The negatively charged surfaces are found on uncharged PEO amphiphilic copolymers[15]. Therefore, the negative value of the zeta potential demonstrates the better dynamic stability of the PFPC and CUR-PFPC mixed nanomicellar formulations.

The CUR-PFPC mixed nanomicellar formulation was characterized by TEM and exhibited an average diameter of ~75 nm. The TEM micrograph presented in Figure 4.5

confirmed the spherical shape of CUR-PFPC nanoformulation. The large gap between adjacent micellar particles was observed in CUR-PFPC, resulting from electrostatic repulsion as well as steric hindrance. The presence of larger sizes of spherical micelles can explain the significant interaction between the Pluronics-PC and the CUR.

4.3.2.2 CUR compatibility and stability in mixed micellar formulation investigation

FTIR, XRD, and DSC studies investigated the physicochemical interactions between the mixed micellar formulation components and the CUR. This interaction is crucial for better drug biocompatibility in nanovesicles.

The FTIR spectra of CUR, PFPC, and CUR-PFPC mixed nanomicellar formulations are shown in Figure 4.6(a). The PFPC spectra displayed significant peaks at 2871 cm^{-1} and 1112 cm^{-1}, corresponding to -C-H stretching and the C-O-C stretching of the aliphatic chain, respectively. The principal characteristic peaks of CUR at 1512 cm^{-1}, 1279 cm^{-1}, and 1158 cm^{-1} result in C=O, C-C, and C-O-C of the -OH group hybridized with the $–OCH_3$ group[38]. Other firm peaks at 1509 cm^{-1}, 965 cm^{-1}, and 725 cm^{-1} confirmed the stretching vibration C=C of the symmetric aromatic ring, -C-H vibration(trans) benzoate, and -C-H vibration(cis) of the aromatic ring, respectively. All the characteristics peaks of CUR and PFPC showed in the spectrum of the CUR-PFPC nanoformulation. Therefore, the absence of a peak of CUR at 1512.55 cm^{-1} can be counted as a CUR being entrapped in the PFPC micellar core instead of attachment to the particle surface. This clarifies the possible interaction between CUR and PFPC in CUR-PFPC, along with the compatibility of CUR in the lipophilic core of the PFPC mixed micelles.

The XRD method helps determine the physical properties of drug-polymer combinations. After analysis, figure 4.6(b) compares the XRD patterns of CUR, PFPC, and CUR-PFPC nanoformulations. Pure CUR displays high intensity and clear crystalline peaks between 10° and 30° (2θ) regions, indicating crystalline in nature[39]. The presence of only two intense peaks of the PEO groups in the XRD pattern of the PFPC formulation at 2θ angles of 19.18° and 23.30° suggested the non-crystalline nature of the mixed micellar formulation[27]. Similar to the PFPC, the optimized CUR-PFPC nanoformulation had the same intensity peaks and flat patterns, indicating the typical non-crystalline nature of the formulation. The intensity of the peak is directly proportional to the crystalline form of the system. Here, CUR-PFPC showed a specific amorphous pattern with a total absence of the

number of classified peaks of CUR, indicating that CUR was molecularly dispersed in a non-crystalline state in the mixed micelles[40] and confirmed the encapsulation of CUR in the PFPC micelles. Thus, increasing solubility, good percentage release, and faster dissolution are ideal aspects of a drug delivery carrier.

Figure 4.6(c) depicts the DSC curves of CUR, PFPC, and CUR-PFPC; CUR shows an endothermic peak (Tm) at 175°C [41], corresponding to the melting point of CUR, and corroborates its crystallinity. The PFPC showed an endothermic melting peak at 52.46˚C, considering the relaxation peak that corelates the melting or Tg of the polymers[14]. The CUR-PFPC thermogram was somewhat similar to PFPC with the reduction in intensity and complete disappearance of the peak at near 175˚C, the melting temperature of CUR. The vanishing of the characteristic melting endothermic peak of CUR usually proves the incorporation of CUR in the mixed micelles. Therefore, it confirmed that CUR was present in a non-crystalline or molecular state in the CUR-PFPC nanoformulation.

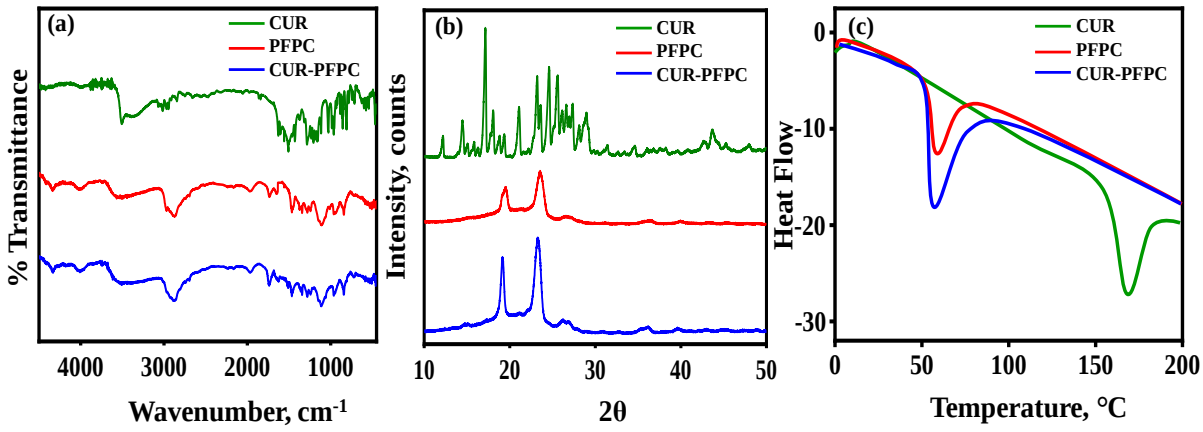

Figure 4.6: (a) FTIR spectrums, **(b)** XRD pattern, and **(c)** DSC thermograms of pure CUR, PFPC and CUR-PFPC formulations

Stability studies of formulations are necessary for daily use and thinking about industrial production. To grant a long shelf-life, stored the CUR-PFPC mixed nanomicellar formulation at RT in dark for 30 days (Figure 4.7). During the storage time, the physical properties remained almost constant. There are not any considerable changes in drug content. Slight drug retention was observed with time, but it is still mono-dispersed. There are no significant changes like turbidity and separation of any layers and no considerable drug

retention in one month. Such observations suggest that CUR-PFPC showed substantial stability.

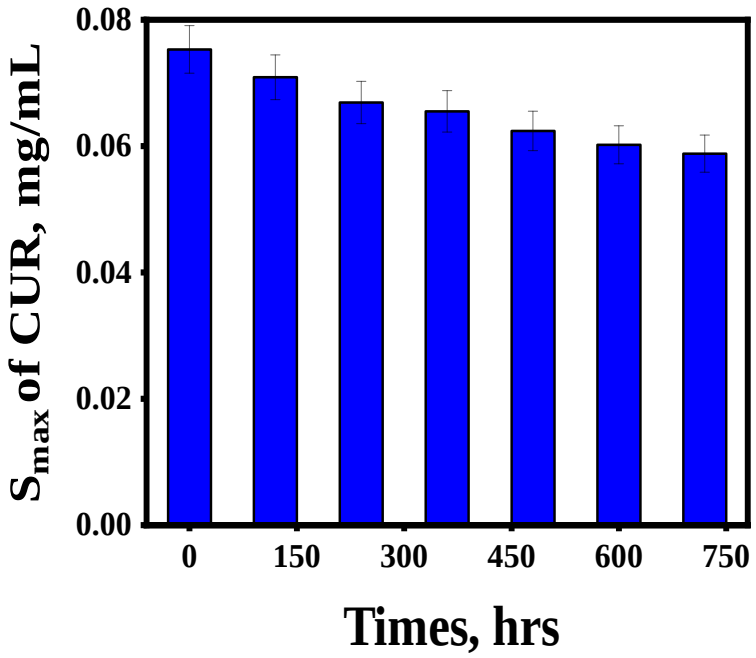

Figure 4.7: Storage stability of optimized CUR-PFPC formulation at 30°±0.5° C.

4.3.3 *In-vitro* biological investigations

4.3.3.1 In-vitro release study

Drug release affects the particle size, drug loading, and drug incorporation into the drug carriers. For successful drug bioavailability, it is significant that drugs incorporated into micellar formulations retain the drug for a specific period after delivery. The *in-vitro* release study of CUR and CUR-PFPC nanoformulations was performed at a physiological pH of 7.4 using the dialysis diffusion bag method. CUR is brilliant yellow and not dissolved in water. So, CUR was solubilized in propylene glycol (PG) solution as a free CUR solution for the drug release study. Figure 4.8 (a) shows that most CUR was released within 24 h, suggesting that CUR could facilely diffuse from the dialysis membrane [19]. Only 30% of CUR was released from the CUR-PFPC nanoformulation during the same period, much slower than the free CUR solution. At the end of the analysis, ~70% of CUR had been released from the formulation. This result shows that the mixed micellar carrier dissolved the hydrophobic CUR drug and sustained the release of CUR. The study revealed that incorporating

hydrophobic CUR had much interaction with the mixed micelles due to PPO and a PC-based core of the mixed micellar formulation.

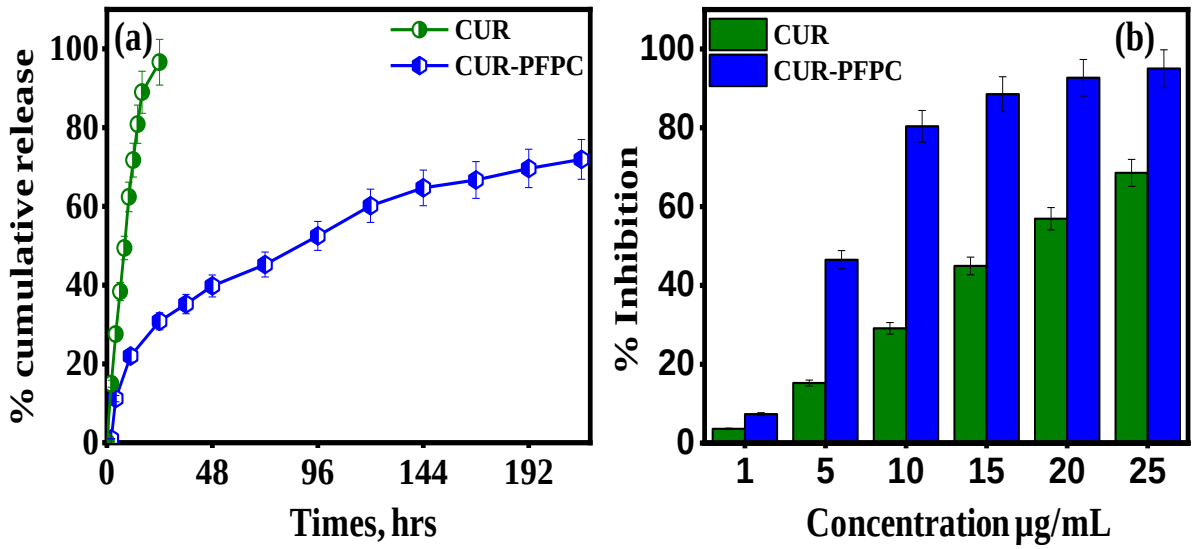

Figure 4.8: (a) *In-vitro* % cumulative release profile of pure CURand CUR-PFPC formulation at 30°±0.5° C and **(b)** %DPPH inhibition of pure CUR drug and CUR-PFPC formulationat various concentrations.

4.3.3.2 In-vitro antioxidant activity

Free radicals like DPPH play a significant role in the oxidative damage of bio-systems[42]. The ability of free CUR (suspended in alcohol) and CUR-PFPC nanoformulation to resist oxidation was tested by comparing DPPH scavenging activity. At 10.0 µg/mL, the maximum scavenging rate of CUR was nearly 89%, whereas CUR-PFPC inhibited almost 96%, as shown in Figure 4.8(b). The change in scavenging activity could improve the CUR antioxidant ability in the mixed micellar formulation. The CUR-PFPC mixed nanomicellar formulation resulted in smaller particle size and better solubility, which enhanced the neutralization of the DPPH radicals and the antioxidant effect of the drug. The antioxidant activities of CUR and CUR-PFPC nanoformulation confirmed oxidation resistance quite significantly better in mixed micellar formulation than in the free drug.

4.3.3.3 In-vitro antimicrobial activity

Antimicrobial drug resistance is one of the most common problems in medical sciences and, therefore, the synergistic effects of antimicrobial agents in blend with biocompatible formulations to develop an antimicrobial mixture with a larger scale of

activity and minimal microbial side effects [43]. The antibacterial activity of the CUR of PFPC mixed micellar nano vehicles showed significant inhibition zone diameter (mm) against each tested bacterial strain.

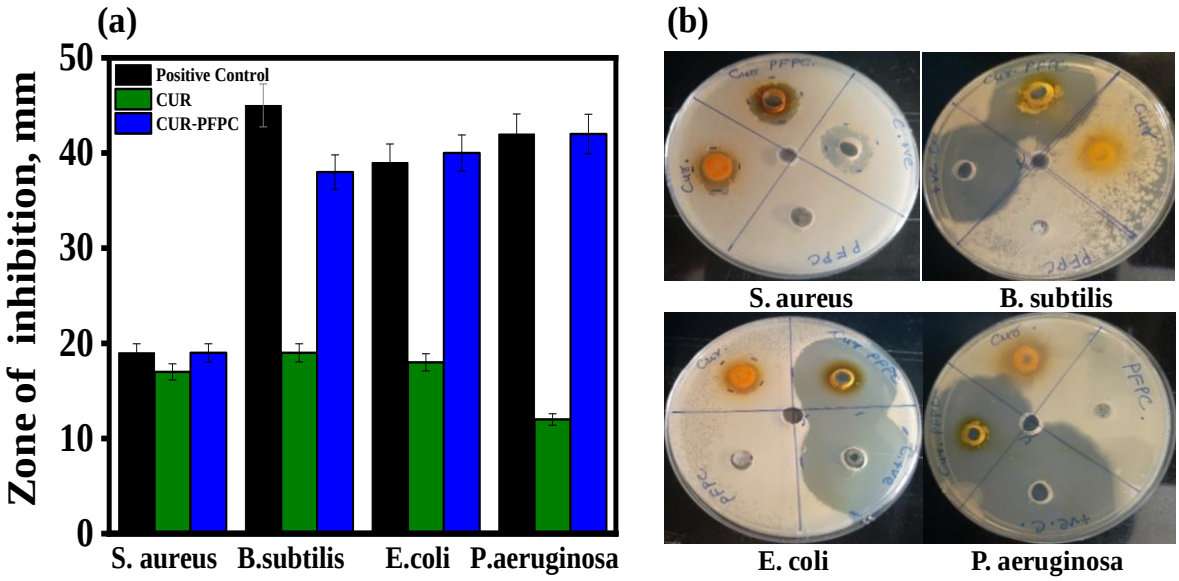

Figure 4.9: Antibacterial activities of pure CUR and CUR-PFPC formulation**(a)** Graphical representation of zone of inhibition against S. aureus, B.subtilis, E.coli and P.aeruginosa **(b)** The photographs of antibacterial activity against S. aureus, B.subtilis, E.coli and P.aeruginosa

Table 4.5 shows the inhibition zones of CUR, PFPC, and CUR-PFPC nanoformulations for clinical and standard bacterial strains of S. aureus and B. subtilis bacteria, as well as gram-negative E. coli and P. aeruginosa bacteria (Figure 4.9(a)).The results suggest that CUR-PFPC has more significant inhibitory effects against bacteria than pure CUR. As shown in Figure 4.9(b), the inhibition zone sizes demonstrated the achievement of a concentration gradient around the spot following CUR release from the CUR-PFPC mixed micelles. The results suggest that CUR-PFPC has significantly more significant inhibitory effects against bacteria than pure CUR. Because of the smaller particle size (67.43 nm) and higher cellular uptake, approaching more damage to the cell membrane of the bacteria compared to CUR (500-800 nm), the improved antibacterial activity [44, 45].

These findings indicate no significant difference in the growth of standard bacterial strains when the antibiotic standard and CUR-PFPC nanoformulation are used. The higher effectiveness of CUR-PFPC nanomicellar systems on bacteria is crucial for curing MDR bacterial infections[46].

Table 4.5. The inhibition zones against bacterial and fungal pathogens

Formulations and standards	Antibacterial activity			
	Zone of inhibition (in mm)			
	Gram +Ve Bacteria		Gram -Ve Bacteria	
	S. aureus	B. subtilis	E.coli	P. aeruginosa
CUR	17.0±0.08	19.0±0.12	18.0±0.09	12.0±0.04
PFPC	00.0	00.0	00.0	00.0
CUR-PFPC	19.0±0.04	38.0±0.12	40.2±0.08	42.0±0.12
Positive control	19.0±0.08	45.0±0.12	39.0±0.12	42.0±0.08
Negative control	00.0	00.0	00.0	00.0
Formulations	**Antifungal activity**			
	Zone of inhibition (in mm)			
	Penicillium	A. niger	S. cereviceae	
CUR	22.0±0.08	13.0±0.02	24.0±0.20	
PFPC	---	---	---	
CUR-PFPC	23.0±0.29	24.0±0.30	26.0±0.08	

Substances and extracts obtained from different ecological resources, mainly plants, have consistently been a potent arsenal for treating fungal infections and spoilage. Because turmeric is widely used in food products, numerous research studies have been conducted to investigate turmeric and curcumin to prevent fungal spoilage and pathogens[47]. The antifungal activities of CUR and CUR-PFPC mixed nanomicellar formulations against Penicillium, *A. niger*, and *S. cerevisiae* fungus stains are presented in Table 4.5. Figure 4.10(a) depicts the size of the inhibition zones of CUR, PFPC, and CUR-PFPC nanoformulations for fungi strains. The zone of inhibition of optimized CUR-PFPC for Penicillium, *A. niger*, and *S. cerevisiae* was 23.0±0.29, 24.0±0.30, and 26.0±0.08 mm, respectively, compared to 22.0±0.08, 13.0±0.02, 300, and 24.0±0.20 mm for CUR. The results show that CUR-PFPC has more inhibitory effects against fungi than pure CUR, as shown in Figure 4.10 images. Here, a considerably higher CUR antifungal activity in mixed micellar formulations is due to the dispersion of CUR in mixed micelles, forming particles with nanometric sizes without any stabilizers.

In both antibacterial and antifungal investigations, the suitable matrixes of biocompatible mixed Pluronics-PC nanomicellar formulations and their water dispersibility and colloidal stability improve antimicrobial activity.

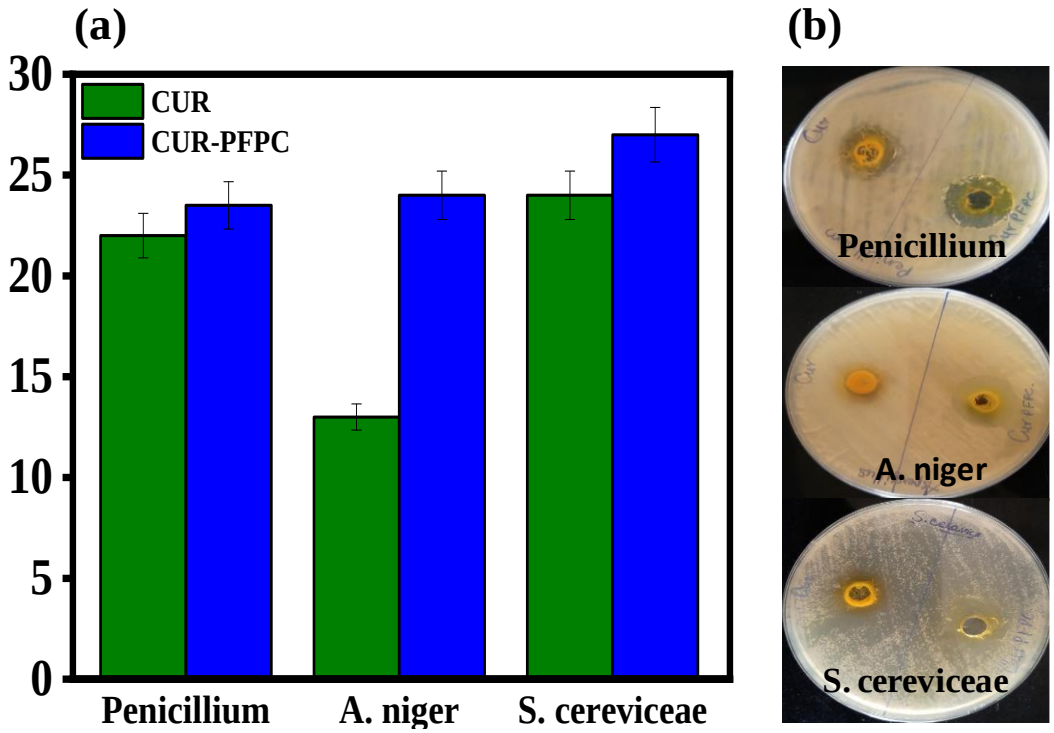

Figure 4.10: Antifungal activities of pure CUR and CUR-PFPC formulation**(a)** Graphical representation of inhibition zone against Penicillium, A.niger, and S.cereviceae and**(b)** The photographs of antifungal activity against Penicillium, A.niger, and S.cereviceae

.

4.4: References

[1] M.C. Fadus, C. Lau, J. Bikhchandani, H.T. Lynch, Curcumin: An age-old anti-inflammatory and anti-neoplastic agent, J. Tradit. Complement. Med. 7 (2017) 339–346.

[2] R. Carolina Alves, R. Perosa Fernandes, B. Fonseca-Santos, F. Damiani Victorelli, M. Chorilli, A critical review of the properties and analytical methods for the determination of curcumin in biological and pharmaceutical matrices, Crit. Rev. Anal. Chem. 49 (2019) 138–149.

[3] L. Yixuan, M.A. Qaria, S. Sivasamy, S. Jianzhong, Z. Daochen, Curcumin production and bioavailability: A comprehensive review of curcumin extraction, synthesis, biotransformation and delivery systems, Ind. Crops Prod. 172 (2021) 114050.

[4] K. Morshedi, S. Borran, M.S. Ebrahimi, M.J. Masoud khooy, Z.S. Seyedi, A. Amiri, M. Abbasi-Kolli, M. Fallah, H. Khan, A. Sahebkar, Therapeutic effect of curcumin in gastrointestinal cancers: A comprehensive review, Phyther. Res. 35 (2021) 4834–4897.

[5] M. Rai, A.P. Ingle, R. Pandit, P. Paralikar, N. Anasane, C.A. Dos Santos, Curcumin and curcumin-loaded nanoparticles: antipathogenic and antiparasitic activities, Expert Rev. Anti. Infect. Ther. 18 (2020) 367–379.

[6] D.P.-A. M Luisa, R.-M. Griselda, M.-L. Valentin, O.-S. Carmina, V.-M. Cristina, M. JJ, G.-T. Maykel, Q.-G. David, S.-S. Roberto, L.-G. Gerardo, Curcumin-loaded poly-ε-caprolactone nanoparticles show antioxidant and cytoprotective effects in the presence of reactive oxygen species, J. Bioact. Compat. Polym. 35 (2020) 270–285.

[7] P. Anand, A.B. Kunnumakkara, R.A. Newman, B.B. Aggarwal, Bioavailability of curcumin: problems and promises, Mol. Pharm. 4 (2007) 807–818.

[8] L. Slika, D. Patra, A short review on chemical properties, stability and nano-technological advances for curcumin delivery, Expert Opin. Drug Deliv. 17 (2020) 61–75.

[9] G. Gaucher, P. Satturwar, M.-C. Jones, A. Furtos, J.-C. Leroux, Polymeric micelles for oral drug delivery, Eur. J. Pharm. Biopharm. 76 (2010) 147–158.

[10] L. Tu, G. Wang, N. Qi, W. Wu, W. Zhang, J. Feng, Multi-functional chitosan

polymeric micelles as oral paclitaxel delivery systems for enhanced bioavailability and anti-tumor efficacy, Int. J. Pharm. 578 (2020) 119105.

[11] E. Tasca, A. Del Giudice, L. Galantini, K. Schillén, A.M. Giuliani, M. Giustini, A fluorescence study of the loading and time stability of doxorubicin in sodium cholate/PEO-PPO-PEO triblock copolymer mixed micelles, J. Colloid Interface Sci. 540 (2019) 593–601.

[12] E. Bernabeu, L. Gonzalez, M. Cagel, E.P. Gergic, M.A. Moretton, D.A. Chiappetta, Novel Soluplus®-TPGS mixed micelles for encapsulation of paclitaxel with enhanced *in vitro* cytotoxicity on breast and ovarian cancer cell lines, Colloids Surfaces B Biointerfaces. 140 (2016) 403–411.

[13] S. Tiwari, V. Kansara, P. Bahadur, Targeting Anticancer Drugs with Pluronic Aggregates: Recent Updates, Int. J. Pharm. 586 (2020) 119544.

[14] G.A. Abdelbary, M.I. Tadros, Brain targeting of olanzapine via intranasal delivery of core–shell difunctional block copolymer mixed nanomicellar carriers: in vitro characterization, ex vivo estimation of nasal toxicity and in vivo biodistribution studies, Int. J. Pharm. 452 (2013) 300–310.

[15] L. Zhao, Y. Shi, S. Zou, M. Sun, L. Li, G. Zhai, N. Li, G. Zhai, Formulation and in vitro evaluation of quercetin loaded polymeric micelles composed of pluronic P123 and Da-tocopheryl polyethylene glycol succinate, J. Biomed. Nanotechnol. 7 (2011) 358–365.

[16] A. Pitto-Barry, N.P.E. Barry, Pluronic® block-copolymers in medicine: from chemical and biological versatility to rationalisation and clinical advances, Polym. Chem. 5 (2014) 3291–3297.

[17] Z. Wei, J. Hao, S. Yuan, Y. Li, W. Juan, X. Sha, X. Fang, Paclitaxel-loaded Pluronic P123/F127 mixed polymeric micelles: formulation, optimization and in vitro characterization, Int. J. Pharm. 376 (2009) 176–185.

[18] R.K. Sharma, S. Shaikh, D. Ray, V.K. Aswal, Binary mixed micellar systems of PEO-PPO-PEO block copolymers for lamotrigine solubilization: a comparative study with hydrophobic and hydrophilic copolymer, J. Polym. Res. 25 (2018) 1–11.

[19] L. Zhao, J. Du, Y. Duan, Y. Zang, H. Zhang, C. Yang, F. Cao, G. Zhai, Curcumin loaded mixed micelles composed of Pluronic P123 and F68: Preparation, optimization

and in vitro characterization, Colloids Surfaces B Biointerfaces. 97 (2012) 101–108.

[20] H.S. Mahajan, V.D. Jadhao, S.M. Chandankar, Pullulan and Pluronic F-127 based in situ gel system for intranasal delivery: Development, in vitro and in vivo evaluation, J. Bioact. Compat. Polym. 35 (2022) 406-418.

[21] S. Fusco, A. Borzacchiello, P.A. Netti, Perspectives on: PEO-PPO-PEO triblock copolymers and their biomedical applications, J. Bioact. Compat. Polym. 21 (2006) 149–164.

[22] E.B. Basalious, R.N. Shamma, Novel self-assembled nano-tubular mixed micelles of Pluronics P123, Pluronic F127 and phosphatidylcholine for oral delivery of nimodipine: in vitro characterization, ex vivo transport and in vivo pharmacokinetic studies, Int. J. Pharm. 493 (2015) 347–356.

[23] B. Dutta, Y.A. Rawoot, S. Checker, S.B. Shelar, K.C. Barick, S. Kumar, R.R. Somani, P.A. Hassan, Micellar assisted aqueous stabilization of iron oxide nanoparticles for curcumin encapsulation and hyperthermia application, Nano-Structures and Nano-Objects. 22 (2020) 100466.

[24] C. Rupp, H. Steckel, B.W. Müller, Solubilization of poorly water-soluble drugs by mixed micelles based on hydrogenated phosphatidylcholine, Int. J. Pharm. 395 (2010) 272–280.

[25] C. Rupp, H. Steckel, B.W. Müller, Mixed micelle formation with phosphatidylcholines: The influence of surfactants with different molecule structures, Int. J. Pharm. 387 (2010) 120–128.

[26] R.L. Duan, X. Sun, J. Liu, T. Gong, Z.R. Zhang, Mixed micelles loaded with silybin-polyene phosphatidylcholine complex improve drug solubility, Acta Pharmacol. Sin. 32 (2011) 108–115.

[27] J. Hao, F. Wang, X. Wang, D. Zhang, Y. Bi, Y. Gao, X. Zhao, Q. Zhang, Development and optimization of baicalin-loaded solid lipid nanoparticles prepared by coacervation method using central composite design, Eur. J. Pharm. Sci. 47 (2012) 497–505.

[28] S.A.A. Radwan, W.H. El-Maadawy, C. Yousry, A.N. ElMeshad, R.A. Shoukri, Zein/phospholipid composite nanoparticles for successful delivery of gallic acid into ahscs: Influence of size, surface charge, and vitamin a coupling, Int. J. Nanomedicine.

15 (2020) 7995.

[29] V.K. Aswal, P.S. Goyal, Small-angle neutron scattering diffractometer at Dhruva reactor, Curr. Sci. 79 (2000) 947–953.

[30] S. Shaikh, D. Ray, V.K. Aswal, R.K. Sharma, Incorporation of Lamotrigine Drug in the PEO–PPO–PEO Triblock Copolymer (Pluronic F127) Micelles: Effect of Hydrophilic Polymers, J. Surfactants Deterg. 20 (2017) 695–706.

[31] B. Gabriele, A. Fazio, M. Carchedi, P. Plastina, In vitro antioxidant activity of extracts of Sybaris liquorice roots from Southern Italy, Nat. Prod. Res. 26 (2012) 2176–2181.

[32] P.K. Mukherjee, R. Balasubramanian, K. Saha, B.P. Saha, M. Pal, Antibacterial efficiency of Nelumbo nucifera (Nymphaeaceae) rhizomes extract, Indian Drugs. 32 (1995) 274–276.

[33] J. Varshosaz, M. Tabbakhian, Z. Salmani, Designing of a thermosensitive chitosan/poloxamer in situ gel for ocular delivery of ciprofloxacin, Open Drug Deliv. J. 2 (2008).

[34] A. Bagchi, P. Mukherjee, S. Bhowmick, A. Raha, Synthesis, characterization and antibacterial activity of a novel curcumin metal complex, Int J Drug Dev Res. 7 (2015) 11–14.

[35] S. Swain, R. Parhi, B.R. Jena, S.M. Babu, Quality by design: concept to applications, Curr. Drug Discov. Technol. 16 (2019) 240–250.

[36] H. Mohamadpour, A. Azadi, K. Rostamizadeh, S. Andalib, M.R. Saghatchi Zanjani, M. Hamidi, Preparation, Optimization, and Evaluation of Methoxy Poly (ethylene glycol)-co-poly (ε-caprolactone) Nanoparticles Loaded by Rivastigmine for Brain Delivery, ACS Chem. Neurosci. 11 (2020) 783–795.

[37] H.A. Salama, A.A. Mahmoud, A.O. Kamel, M.A. Hady, G.A.S. Awad, Phospholipid based colloidal poloxamer–nanocubic vesicles for brain targeting via the nasal route, Colloids Surfaces B Biointerfaces. 100 (2012) 146–154.

[38] M.U. Akbar, K.M. Zia, A. Nazir, J. Iqbal, S.A. Ejaz, M. Sajid, H. Akash, Pluronic-Based Mixed Polymeric Micelles Enhance the Therapeutic Potential of Curcumin, 19 (2018).

[39] K. Hu, X. Huang, Y. Gao, X. Huang, H. Xiao, D.J. McClements, Core–shell biopolymer nanoparticle delivery systems: Synthesis and characterization of curcumin

fortified zein–pectin nanoparticles, Food Chem. 182 (2015) 275–281.

[40] S. Ji, X. Lin, E. Yu, C. Dian, X. Yan, L. Li, M. Zhang, W. Zhao, L. Dian, Curcumin-Loaded Mixed Micelles : Preparation , Characterization , and In Vitro Antitumor Activity, 2018 (2018).

[41] F.U. Vaidya, R. Sharma, S. Shaikh, D. Ray, V.K. Aswal, C. Pathak, Pluronic micelles encapsulated curcumin manifests apoptotic cell death and inhibits pro-inflammatory cytokines in human breast adenocarcinoma cells, Cancer Rep. 2 (2019) e1133.

[42] D.K. Jha, L. Panda, S. Ramaiah, A. Anbarasu, Evaluation and comparison of radical scavenging properties of solvent extracts from Justicia adhatoda leaf using DPPH assay, Appl. Biochem. Biotechnol. 174 (2014) 2413–2425.

[43] K. Zandi, E. Ramedani, K. Mohammadi, S. Tajbakhsh, I. Deilami, Z. Rastian, M. Fouladvand, F. Yousefi, F. Farshadpour, Evaluation of antiviral activities of curcumin derivatives against HSV-1 in Vero cell line, Nat. Prod. Commun. 5 (2010) 1934578X1000501220.

[44] M.A. Adahoun, M.-A.H. Al-Akhras, M.S. Jaafar, M. Bououdina, Enhanced anti-cancer and antimicrobial activities of curcumin nanoparticles, Artif. Cells, Nanomedicine, Biotechnol. 45 (2017) 98–107.

[45] R.K. Basniwal, H.S. Buttar, V.K. Jain, N. Jain, Curcumin nanoparticles: preparation, characterization, and antimicrobial study, J. Agric. Food Chem. 59 (2011) 2056–2061.

[46] P.A. Smith, M.F.T. Koehler, H.S. Girgis, D. Yan, Y. Chen, Y. Chen, J.J. Crawford, M.R. Durk, R.I. Higuchi, J. Kang, Optimized arylomycins are a new class of Gram-negative antibiotics, Nature. 561 (2018) 189–194.

[47] R.S. Upendra, P. Khandelwal, A.H.M. Reddy, Turmeric powder (Curcuma longa Linn.) as an antifungal agent in plant tissue culture studies, Int. J. Eng. Sci. 3 (2011) 7899–7904.